Thermal Decomposition of Dimethylnitramine and Dimethylnitrosamine by Pulsed Laser Pyrolysis

S. Esther Nigenda, Donald F. McMillen, and David M. Golden*

Department of Chemical Kinetics, SRI International, Menlo Park, California 94025
(Received: November 30, 1987)

Pyrolysis of dimethylnitramine (DMNA) and dimethylnitrosamine (DMNO) was carried out in a flow system over the temperature range 800–900 K using pulsed infrared laser heating, via SF_6 in a 250-Torr bath of CO_2 and radical scavenger. Arrhenius parameters for DMNO and DMNA composition were $\log k\ (s^{-1}) = (15.8 \pm 1.1) - (50.0 \pm 3.4)/2.3RT$ and $(13.5 \pm 0.6) - (37.4 \pm 2.5)/2.3RT$, respectively. The former set of parameters is consistent with simple bond scission as the rate-limiting step; the latter set, which was produced with different scavengers, temperature standards, and varying amounts of added NO as a radical trap, is not consistent with simple bond scission. The experimental results can be reproduced via a mechanistic numerical model in which N–NO_2 bond scission and nitro–nitrite rearrangement are competitive initial steps and the displacement of NO_2 from DMNA by NO is included as a low-temperature route to DMNO.

Introduction

Some years ago Fluornoy[1] reported that the decomposition of *N,N*-dimethylnitramine in static bulb experiments over the temperature range 165–200 K resulted in formation of *N,N*-dimethylnitrosamine in roughly 80% yield. He explained this product via recombination of NO and dimethylamino radicals. This reaction is in itself completely reasonable. However, Fluornoy found it necessary to invoke reactions that would produce NO in high yield, but these are somewhat vague and questionable, as discussed by Lin.[2] Several years ago, we[3] used the very low pressure pyrolysis technique (VLPP) to examine dimethylnitramine decomposition at pressures in the milliTorr range. More recently, Lin and co-workers have studied the decomposition of dimethylnitramine in both low-temperature (466–524 K) static bulb experiments[2] and in single-pulse shock tube work at much higher temperatures (800–1200 K).[4] Lee and co-workers[5] have also recently studied the infrared multiphoton decomposition of dimethylnitramide under collisionless conditions. The results of these and other workers are summarized in Table I. In all but the two cases where the molecules are the most isolated (the multiphoton and the VLPP studies), the major product is dimethylnitrosamine. Thus, reaction leads to a product having the N–N bond intact, in spite of the fact that the initial reactions are presumed to have involved N–N bond scission of one sort or another. Re-forming the N–N bond (e.g., through radical recombination with NO) is not in itself difficult, but for it and other secondary reactions to take place at rates such that dimethylnitrosamine is produced in almost quantitative yield is a result that one would not have predicted.

The general goal of this work is to determine the products of dimethylnitrosamine decomposition and the temperature dependence of the various rate-controlling processes, in order to help achieve the overall goal of understanding what controls the decomposition of cyclic nitramines and other energetic materials. Under almost all circumstances (all but low concentrations and/or very short time scales), the nature of these materials dictates that this means considering not only the initial steps but also a varying range of secondary reactions. This paper presents our results for the thermal decomposition of dimethylnitramine and dimethylnitrosamine using GC–MS monitored laser-powered homogeneous pyrolysis (LPHP). In this technique, the net decomposition in a flow system averaged over many laser pulses and over the entire volume of the cell is measured. A mechanistic numerical model accounting for the observed Arrhenius parameters, the products, and their relative yields is also presented. Complementary results obtained with a real-time molecular beam mass spectrometrically monitored version of LPHP are the subject of a paper to be submitted.

TABLE I: Literature Parameters for Dimethylnitramine Decomposition

log (A/s^{-1})	E, kcal/mol	technique	T range, K	P, Torr	ref/year
a	*a*	mol beam MPD	*a*	*a*	5/1986
15.9	44.1	bulb/SPST	466–1000	474, 3–6	4/1985
16.5 ± 0.5	45.4	bulb	466–524	475	2/1985
12.4	37.0	VLPP	560–850	$\sim 10^{-3}$	3/1979
13.7	38.9	bulb	450–510	~200	6/1987
14.1	40.8	bulb	450–530	64–400	7/1964
20.1	53.0	bulb	440–470	200–750	1/1961

[a] Product mass spectra and flight times consistent with N–NO_2 band scission.

Experimental Procedure

The pulsed laser pyrolysis technique used here (GC–MS monitored) has been described in detail.[8] Briefly, a CO_2 laser is used to heat the substrate (at 0.1 Torr) via an absorbing but unreactive gas (e.g., SF_6, ~10 Torr), which then transfers its kinetic energy by collision (total pressure 100 Torr, collision frequency 10^9/s), bringing the substrate to high temperature in 1–3 μs. For radical-forming processes, scavengers and/or traps are necessary (e.g., toluene, cyclopentane, NO, ~5–20 Torr). Reaction then occurs in the roughly 10 μs available before cooling takes place as the acoustic expansion wave moves radially inward toward the center of the cell. Figure 1 shows a schematic of the LPHP apparatus.

With the LPHP technique, surface-catalyzed reactions at high temperatures are essentially precluded, since the time scale for heating, reaction, and cooling is far shorter than the millisecond time scale of diffusion to the walls. (Adsorption of IR-absorbing reactants or products on the KCl windows could conceivably result in decomposition of an adsorbed phase. This is generally unlikely, since only extremely strongly absorbing materials would be heated to a sufficiently high temperature when present at only a few monolayers thickness on the transparent, cold windows).

(1) Fluornoy, J. M. *J. Chem. Phys.* **1962**, *36*, 1106.
(2) Lloyd, S. A.; Umstead, M. E.; Lin, M. C. *J. Energ. Mater.* **1985**, *3*, 187.
(3) McMillen, D. F.; Barker, J. R.; Lewis, K. E.; Trevor, P. L.; Golden, D. M. "Mechanisms of Nitramine Decomposition: Very Low-Pressure Pyrolysis of HMX and Dimethylnitramine", Final Report, SRI Project PYU-5787, June 18, 1979 (SAN 0115/117). DOE Contract EY-76-C-03-0115.
(4) Umstead, M. E.; Lloyd, S. A.; Lin, M. C. In *Proceedings of the 22nd JANNAF Combustion Meeting*; CPIA: 1985; p 512.
(5) Wodtke, A. M., private communication.
(6) Korsunskii, B. L.; Dubovitskii, F. I.; Sitonina, G. V. *Dokl. Akad. Nauk SSSR* **1967**, *174*(5), 1126.
(7) Korsunskii, B. L.; Dubovitskii, F. I. *Dokl. Akad. Nauk SSSR* **1964**, *155*(2), 402.
(8) McMillen, D. F.; Lewis, K. E.; Smith, G. P.; Golden, D. M. *J. Phys. Chem.* **1982**, *86*, 709.

0022-3654/89/2093-1124$01.50/0 © 1989 American Chemical Society

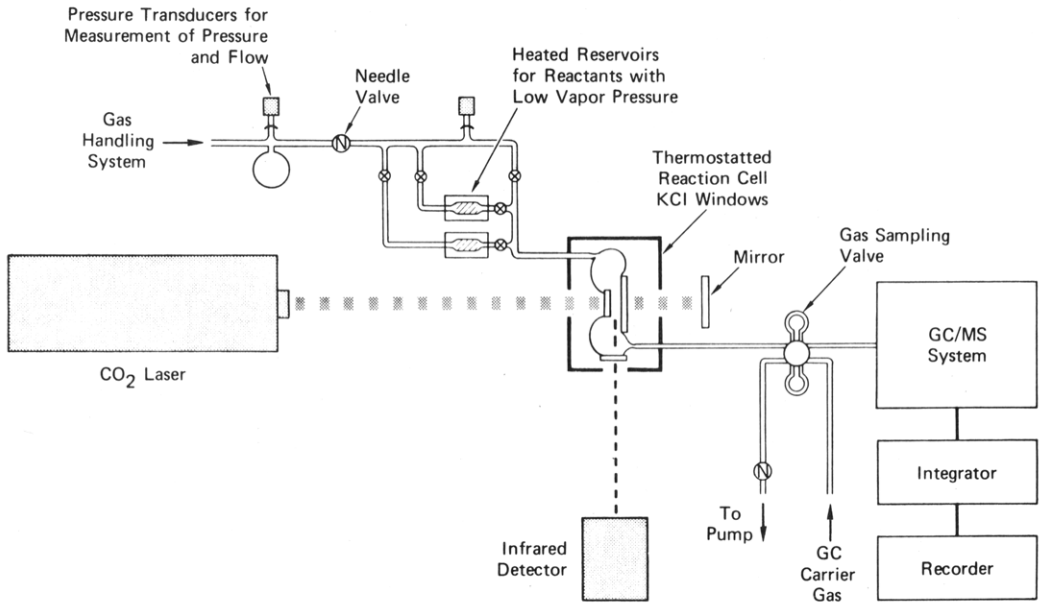

Figure 1. Schematic of GC–MS monitored LPHP apparatus.

The need to explicitly measure the temperature corresponding to any particular measurement of k is eliminated by use of the "comparative rate" technique.[8,9] This involves concurrent determination of the fractional decomposition of a temperature standard, a second "substrate" (~0.2 Torr) whose decomposition rate temperature dependence is already well-known and therefore whose fractional decomposition defines an "effective" temperature that is a convolution of temperature over time and space within the heated portion of the cell. Given that the temperature dependence of the substrate and the temperature standard are not greatly different and that the fractional decomposition of both materials is less than about 25%, the standard and the substrate "track" the temperature variations in a similar manner. Data reduction simply involves determining the slope and intercept of a plot of log $k_{unknown}$ vs log $k_{standard}$, which correspond to the ratio of activation energies and the difference in the log A values, respectively. As discussed in ref 8 and 9, uncertainties in reaction time and in cell volumes cause no error in the derived activation energies (slope of the comparative rate plot) and only small errors in derived A factors.

The extent to which the comparative rate method accommodates the temperature and reaction time variations inherent in this laser pyrolysis technique has been amply demonstrated by estimates of the errors involved and by testing the technique using a series of "unknowns" whose Arrhenius parameters have already been reported in the literature.[8,9d] This has provided values in good agreement with the literature parameters for a series of molecular elimination reactions. The precision achievable indicates that the pulse-to-pulse and minute-to-minute laser variations that existed under the conditions of this experiment did not give rise to any distortion of the derived temperature dependence. Tests of this type make it clear that the comparative rate method, applied to pulsed laser pyrolysis, is very successful in accommodating the temperature variations inherent in the method and thereby providing an accurate measure of the temperature dependence of the substrate.

In this particular study, initial experimental difficulties included adsorption of substrates on the cell walls, premature decomposition of substrates, and interference by chemical impurities. These difficulties were minimized and good mass balances obtained by silanizing the entire flow system including the gas reservoirs, by carefully maintaining the lines and cell temperatures at 95 °C (at lower temperatures, adsorption occurred; at higher temperatures, preliminary decomposition occurred), and by scrupulous purification of all compounds used. In particular, traces of NO_2 were removed from NO by passing it through three scrubbers containing 10 M NaOH, NaOH pellets, and molecular sieves, respectively. Special care was given to the elimination of NO_2 from NO, since the former readily gave rise to the nitrates and nitrites of the temperature standards used, thus distorting their decomposition temperature dependence.

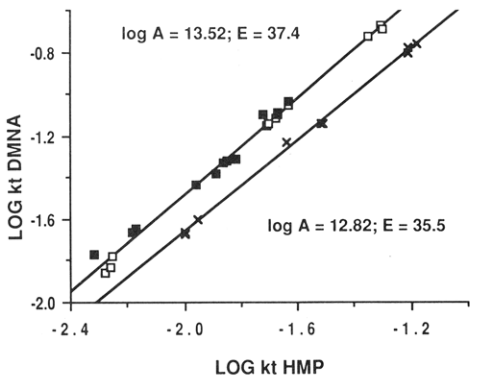

Figure 2. Comparative rate plot of dimethylnitramine (DMNA) vs 4-hydroxy-4-methyl-2-pentanone (HMP): (■) 50-fold excess of NO; (□) 100-fold excess of NO; (×) no additional NO; toluene as scavenger.

Results

Experiments. The thermal decomposition of dimethylnitramine was studied over the temperature range 780–880 K. Figure 2 shows the decomposition rate of dimethylnitramine versus that of 4-hydroxy-4-methyl-2-pentanone (HMP) for two different experimental conditions. The rate expression[10] for HMP is log k (HMP → 2-acetone) = $11.63 - 32.3/2.3RT$. In most cases an approximately 50- to 100-fold excess of radical scavenger, i.e., either toluene or cyclopentane, was used and the mass balance (decomposed material accounted for as product) for the temperature standard was 99 ± 3%.

Excess nitric oxide was used in two of the runs shown in Figure 2 in order to trap any dimethylaminyl radicals formed by the homolysis of the N–N bond in dimethylnitramine. Secondary reactions and products were thus minimized, and dimethylnitrosamine accounted for 100 ± 16% of the decomposed dimethylnitramine (for decompositions that were typically less than 10%). The least-squares line drawn through the filled and unfilled

(9) (a) Tsang, W. *J. Chem. Phys.* **1964**, *40*, 1171. (b) Tsang, W. *Ibid.* **1964**, *41*, 2487. (c) Tsang, W. *Ibid.* **1967**, *46*, 2817. (d) Shaub, W. M.; Bauer, S. H. *Int. J. Chem. Kinet.* **1975**, *7*, 509.

(10) Smith, G. G.; Yates, B. L. *J. Org. Chem.* **1965**, *30*, 2067.

TABLE II: Laser Pyrolysis Comparative Rate Results for Dimethylnitramine

temp std	scavenger	x-fold excess of NO	log (A/s^{-1})	E_a, kcal/mol	nitrosamine yield[a]
HMP	cyclopentane	100	13.5	37.7	113
HMP	toluene	100, 50	13.9	38.0	99
HMP	toluene	0	12.8	35.5	25

[a] (dimethylnitrosamine)/Δ(dimethylnitramine).

squares is a composite of two runs performed under similar conditions. Toluene was used as the radical scavenger with a 50-fold excess of nitric oxide in one run (filled squares) and a 100-fold excess in the other (unfilled squares). As shown in Table II, the Arrhenius parameters for the dimethylnitramine decomposition in the presence of excess NO, with either toluene or cyclopentane as the radical scavenger, are essentially the same, i.e., log k (s^{-1}) = 13.5 ± 0.6 − (37.4 ± 2.5)/2.3RT.

Data obtained with toluene as the scavenger and in the absence of nitric oxide are also plotted in Figure 2. In this case no more than 60% of the decomposed dimethylnitramine could be accounted for, appearing as dimethylnitrosamine (25%), methylmethylenimine (~20%), nitrous acid (~12%), dimethylamine (~8%), and *N,N*-dimethylbenzylamine (~3). These yields varied with temperature, with the dimethylnitrosamine yield being smaller at the lower end of the temperature range. Trace amounts of *N,N*-dimethylacetamide were tentatively identified. Unlike runs with excess NO, in which virtually identical comparative rate plots are obtained from either reactant disappearance or product appearance, the comparative rate plot for data obtained in the absence of excess NO could only be based on the amount of dimethylnitramine lost. Nevertheless, as shown in Figure 2 and in Table II, the Arrhenius parameters obtained for dimethylnitramine decomposition in the absence of excess nitric oxide are still similar to those obtained in its presence.

Prior to the use of HMP as the temperature standard in the thermal decomposition of dimethylnitramine, *tert*-butyl bromide was used as the temperature standard[11] in several runs in which the nature of the radical scavenger or of the nitrogen oxide present in the gas mixture was varied. The Arrhenius parameters obtained from the resulting comparative rate plots were similar to those obtained with HMP. However, due to experimental difficulties (see Experimental Section), attempted mass balances for both the temperature standard and the dimethylnitramine ranged widely. The quantitative results were therefore considered unreliable and are not reported here (even though the Arrhenius parameters generally fall within the range shown in Table II). The following qualitative observations from these runs are nonetheless considered pertinent in understanding this system's complexities, and we attempted to incorporate them in the mechanistic modeling of the DMNA decomposition.

In the absence of excess nitrogen oxides, use of toluene as a radical scavenger resulted in the formation of *N,N*-dimethylbenzylamine, benzene, and bibenzyl in addition to the formation of *N,N*-dimethylnitrosamine as the major product and formaldehyde in trace amounts. Use of cyclopentane as the radical scavenger gave, in addition to nitrosamine and formaldehyde, nitrocyclopentane and cyclopentene.

Since the reduction of NO_2 in secondary reactions is considered to be a critical step in dimethylnitrosamine production via recombination of the dimethylamino radical with NO, dimethylnitramine decomposition was also studied in the presence of toluene, *tert*-butyl bromide, and roughly a 100-fold excess of nitrogen dioxide. Although a temperature standard was not included in this run, excess NO_2 appeared to have no substantial effect on the dimethylnitramine decomposition rate.

When the dimethylnitramine decomposition was carried out in the absence of radical scavenger or of nitrogen oxides, dimethylnitrosamine continued to be the major product, but formaldehyde was produced in more than 50% yield (relative to nitrosamine produced), and the rate of nitramine loss apparently increased by a factor of from 2 to 5. (The exact extent of acceleration is uncertain because the temperature standard was also absent in these runs.)

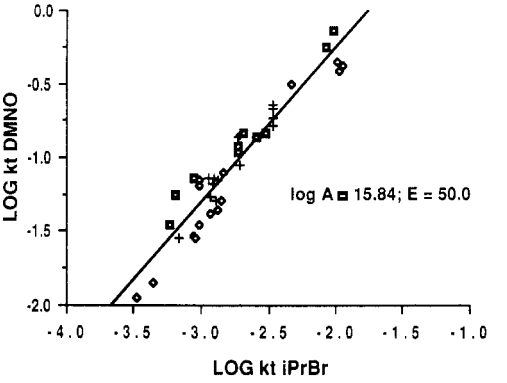

Figure 3. Comparative rate plot of dimethylnitrosamine (DMNO) vs isopropyl bromide (*i*-PrBr). (The different symbols represent experiments on different days.)

In order to check the behavior of our temperature standard, HMP, its Arrhenius parameters were independently determined by using the LPHP comparative rate technique with *t*-butyl bromide as the temperature standard (literature parameters[11] log k/s^{-1} = 13.8 − 41.8/2.3RT). The A factor and activation energy for HMP thus determined were in excellent agreement with those reported in the literature[10] (log A = 11.9 vs 11.6 and E_a = 32.9 vs 32.8 kcal/mol, respectively). This result, along with the good mass balances obtained for dimethylnitramine decomposition in the presence of excess nitric oxide and the similar Arrhenius parameters found for dimethylnitramine with *tert*-butyl bromide as the temperature standard, all suggest that the Arrhenius parameters we report for dimethylnitramine are not distorted by systematic errors resulting from different temperature tracking behaviors.

Because of its importance as a product, the thermal decomposition of dimethylnitrosamine was also studied over the temperature range 870–990 K, with isopropyl bromide as the temperature standard. The comparative rate plot is shown in Figure 3. With dimethylnitrosamine the sequence of secondary gas-phase reactions is considerably simpler than with dimethylnitramine since the formation of imine by loss of a hydrogen atom is, in the presence of scavenger, essentially irreversible, and the sequence of oxidation steps that takes place when NO_2 is present cannot occur here. However, GC analysis of the imine presents a problem, since the proclivity of imines for polymerization reactions means that any surface contacted by the imine (e.g., in the heated transfer lines) is a candidate for promoting polymerization. The extent of this polymerization varies from day to day, exhibiting a sensitivity to factors not easily defined. Samples of the gummy polymer were collected and subjected to analysis by field ionization mass spectrometry (FIMS). The dominant peak in the pyrolysis/FIMS spectra of this material was m/z 86, corresponding to an imine dimer produced from thermal decomposition of the imine polymer.

The net result of this behavior is that, although the gas-phase secondary reactions of dimethylnitrosamine are much simpler than for dimethylnitramine, reliable quantitative product analysis is very difficult. Hence, the kinetics were based solely on DMNO disappearance, and there is substantial scatter in the comparative rate plot. This scatter notwithstanding, the parameters extracted from the data in Figure 3 are consistent both with the expectation of simple N–NO bond scission as the rate-limiting step and with the BAC-4 calculations of Melius[12] that suggest N–NO bonds

(11) Tsang, W. *J. Chem. Phys.* **1964**, *40*, 1498.

(12) Melius, C. F.; Binkley, J. S. In *Proceedings of the 21st Symposium (International) on Combustion*, 1987; The Combustion Institute: Pittsburgh, PA, 1988; p 1953.

TABLE III: Parameters Used in Numerical Modeling of Dimethylnitramine and Dimethylnitrosamine Decomposition

no.	reaction	log A^a	E, kcal/mol
1	$(CH_3)_2N-NO_2 \rightarrow (CH_3)_2N + NO_2$	15.3	46.5
2	$(CH_3)_2N-NO_2 \leftarrow (CH_3)_2N + NO_2$	8.8	-2.0
3	$(CH_3)_2N-NO_2 \rightarrow (CH_3)_2N-O-N=O$	11.5	31.0
4	$(CH_3)_2N-NO_2 \leftarrow (CH_3)_2N-O-N=O$	10.5	11.1
5	$(CH_3)_2N-ON=O \rightarrow (CH_3)_2N-O^\bullet + NO$	13.7	9.0
6	$(CH_3)_2N-O-N=O \leftarrow (CH_3)_2N-O^\bullet + NO$	9.9	0.0
7	$(CH_3)_2N^\bullet + NO_2 \rightarrow (CH_3)_2N-O^\bullet + NO$	10.0	0.0
8	$(CH_3)_2N^\bullet + NO_2 \leftarrow (CH_3)_2N-O^\bullet + NO$	9.9	13.8
9	$(CH_3)_2N^\bullet + NO \rightarrow (CH_3)_2N-NO$	9.8	-2.0
10	$(CH_3)_2N^\bullet + NO \leftarrow (CH_3)_2N-NO$	15.5	50.3
11	$(CH_3)_2N-O-N=O + NO \rightarrow (CH_3)_2N-NO + NO_2$	9.7	5.0
12	$(CH_3)_2N-NO_2 + H^\bullet \rightarrow (CH_3)_2N-NO + OH^\bullet$	10.0	0.0
13	$(CH_3)_2N-NO_2 + CH_3^\bullet \rightarrow (CH_3)_2N-NO + CH_3O$	9.0	0.0

[a] Units of A are s^{-1} and L/(m s) for unimolecular and bimolecular reactions, respectively.

DMNA DECOMPOSITION MECHANISM

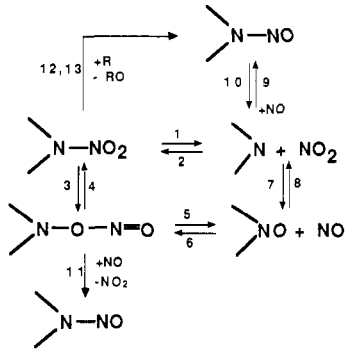

Figure 4. Schematic representation of the mechanism at DMNA decomposition in the presence of excess NO.

are *not* weaker than their N–NO_2 counterparts, in marked contrast to C–NO bonds and their C–NO_2 counterparts.[13] Thus, this result serves to reiterate that the LPHP technique behaves as claimed and impels us to examine the chemistry more closely in the case of dimethylnitramine.

Numerical Modeling. In considering the data presented above, the goal was to choose a sequence of reactions that (1) explained the observed products and the relative yield in which they are formed, (2) explained the observed overall rate parameters, and (3) did so with known or plausible parameters for each of the elementary processes. The mechanistic numerical model we constructed to help explain the results (decomposition of dimethylnitramine) consists of 75 primary and secondary reactions that account for all of the observed products. Reverse reactions were initially included for all reactions; some were dropped from the model when thermochemically limited parameters and numerical integration showed them to be of negligible importance. Certain reactions postulated in the literature as important contributors for the dimethylnitramine decompostion were retained in the model even if thermochemical limitations ruled out their importance.

The Arrhenius parameters for all reactions were taken from the literature where possible; otherwise, they were derived by estimation teqhniques from analogous reactions in the literature. Where appropriate, the degree of falloff was estimated by the RRK method. Instead of discussing each reaction and the parameters used for it individually, the main reactions in the model are schematically depicted in Figure 4. In Table III we list the rate parameters for the reactions included in Figure 4. We have

MODEL RESULTS

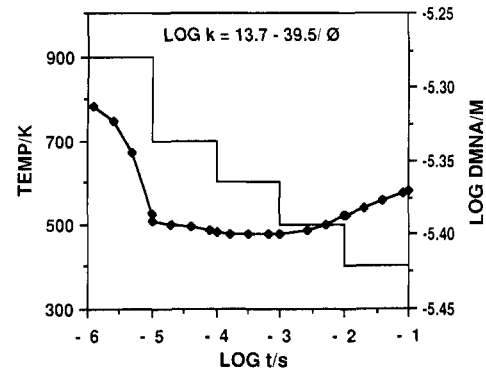

Figure 5. Schematic representation of the temperatures changes with time imposed during numerical modeling to represent LPHP conditions. Also shown is the computed variation of DMNA with time. Initial conditions for model: cell temperature 367 °C, P_0(DMNA) = 0.11 Torr, P_0(*o*-fluorotoluene), P_0(NO) = 5.7 Torr, P_0(hydroxymethylpentanone) = 0.11 Torr.

endeavored to assure maximum utility for the modeling effort by remaining cognizant of the fact that literature data[14] for all of the reaction types allow only a limited range within which the parameters can be varied without pressing the limits of plausibility.

In order to approximate the physical characteristics of the LPHP system and to account for the possibility of reaction during cooling (primarily low activation energy secondary reactions of radicals) of the laser-heated portion of the cell, the model incorporated a drop of 200 K (from the initial 900 K) at the end of the first time decade (10 μs), followed by 100 K drops at the end of each succeeding decade. The sequence of differential equations provided by the reactions was then integrated over time and temperature by a program that uses a numerical integration routine based on the Gear algorithm. The temperature profile and the computed dimethylnitramine concentration as a function of time are shown in Figure 5.

The experimental temperature dependence and product yields under different conditions were successfully reproduced only when the model included the nitro–nitrite rearrangement and also reactions 4, 6, and 11. These reactions are reversal of the nitro–nitrite rearrangement, reversal of the nitrite thermolysis, and displacement of NO_2 from the nitrite by NO, respectively. The reasonableness of these reactions is considered in the following section; taken at face value, the computed values suggest that the experimental results do in fact reflect initial competition between simple bond scission and nitro–nitrite rearrangement, each with the parameters shown in Table III.

Discussion

As described in the preceding section, the mechanism whose important elements are shown in Figure 4 is able to reproduce the data, including nitramine decomposition rate parameters and dimethylnitrosamine yield under a range of experimental conditions, and furthermore does so with rate parameters for the various steps that are either experimentally determined or plausible extrapolations from related reactions. In this section, we examine the key steps in the model and discuss them relative to those that have been suggested in previous studies to account for observed rates and products.

The basic experimental results that must be duplicated if a dimethylnitramine decomposition mechanism is to be considered potentially valid are the decomposition rate and dimethylnitrosamine yield as a function of temperature and radical scavenger/trap concentrations. The difficulty that this seemingly simple requirement presents is that the experimental parameters are too low for simple bond scission to be the dominant rate-determining step, but any molecular elimination or rearrangement pathway that one writes to allow duplication of the Arrhenius parameters does not lead, by a simple sequence of known reactions, to the observed dimethylnitrosamine yields. Specifically, such sequences do not provide a route from the nitroxyl radical (which is the

(13) McMillen, D. F.; Golden, D. M. *Annu. Rev. Phys. Chem.* **1982**, *33*, 497.

(14) See, for example: Kerr, J. A.; Moss, S. J. *CRC Handbook of Bimolecular and Termolecular Gas Reactions*; CRC Press: Boca Raton, FL, 1981; Vols. 1 and 2. Tsang, W.; Hampson, *J. Phys. Chem. Ref. Data* **1986**, *15*, 1087–1279.

unavoidable scission product that follows nitro–nitrite rearrangement) to the nitrosamine. (One might have imagined that HONO from molecular elimination could take part in some surface-promoted nitrosation of amine during transport of the reaction products to the GC–MS system, but this would have involved reaction with the amine rather than the imine. Furthermore, the imine tends to undergo a variable amount of polymerization on the walls of the transfer lines; the observed yield of dimethylnitrosamine is quite reproducible and therefore not easily connected with reactions subject to variations in surface conditions.)

Given the notorious susceptibility of even precisely measured Arrhenius parameters to distortion by systematic error, we were initially inclined to assign the low-temperature dependence to such distortions and conclude that the 100% yield of nitrosamine produced in the presence of excess NO simply resulted from trapping a quantitative yield of dimethylamino radicals produced in an initial N–NO_2 bond scission. However, the rate measurements made under a wide range of experimental conditions that were employed in an effort to minimize distortion of the temperature dependence by spurious secondary reactions have repeatedly given $\log k\ (s^{-1}) = 13.5 \pm 0.6 - (37.4 \pm 2.5)/2.3RT$, as described in the preceding section. Furthermore, we conclude that there is no significant distortion of the temperature dependence by the highly reactive imine, since pyrolysis of dimethylnitrosamine, which yields the imine as the dominant product, produces a temperature dependence completely consistent with an N–NO bond scission. [Finally, preliminary results of dimethylnitramine pyrolysis in a molecular beam mass spectrometrically sampled LPHP cell reveal that mass 60 and mass 30 (presumably dimethylnitroxyl radical and NO) are products of an initial unimolecular decomposition step.] Thus, the results indicating that a low A factor initial step contributes to dimethylnitramine decomposition became too consistent to simply reject out of hand and demanded a plausible mechanism that could account for them.

The critical reactions that make it possible for the numerical model to duplicate the low Arrhenius parameters and high dimethylnitrosamine yields in the presence of excess NO are shown in Figure 4 and Table III, which have been abridged for purposes of discussion. The critical elements are the following:

1. N–NO_2 bond scission and NO_2–ONO rearrangement that are roughly competitive at 900 K (reactions 1 and 3).
2. Rapid, but *reversible*, thermolysis of the very weak O–NO bond in the *N*-nitrite (reactions 5 and 6).
3. Reverse of the nitro–nitrite rearrangement (reaction 4).
4. Attack of NO on the *N*-nitrite to displace NO_2 and yield directly the nitrosamine (reaction 11).

The reverse reactions of the nitro–nitrite rearrangement and of the nitrite thermolysis are required by microscopic reversibility (though we did not initially anticipate their impact). Reversal of the O–NO bond thermolysis is important only in the presence of excess NO, and it is only this reversal that can maintain a high enough steady-state concentration of the weakly bonded nitrite such that reversal of the nitro–nitrite rearrangement (reaction 4) becomes significant. It is this latter reaction that allows some return to the nitramine and helps to limit the formation, under these conditions, of other products from the nitroxyl radical.

The only reaction in the sequence without direct precedent is reaction 11, the displacement of NO_2 from the nitrite by NO. This reaction is most important at lower temperatures. Because it is a low activation energy process and it limits return from the nitrite, it serves to substantially increase the net decomposition at low temperatures, while providing an additional route to nitrosamine. As an addition–elimination reaction between a free radical and a substrate having partial double-bond character, it is the type of reaction that could well proceed with a low activation energy. As currently incorporated in the model, it has a 5 kcal/mol activation energy. If this is raised to 10 kcal/mol, the computed overall activation energy for DMNA loss is raised from 39.5 to 44.5 kcal/mol (i.e., 75% of the way to the 46.1 kcal/mol that results from complete elimination of reaction 11). There may conceivably be alternatives to reaction 11; as the reaction sequence is currently written, this reaction constitutes a necessary and reasonable route to nitrosamine from the easily formed nitroxyl radical. That is, if nitrosamine is to be formed from the nitroxyl radical, the oxygen on the nitrogen clearly must depart, and departing as one of the oxygens on an NO_2 seems an eminently reasonable way to accomplish this. It is interesting to note that the stability of the nitroxyl radical at the same time makes it the inevitable product of the nitro–nitrite rearrangement and a bottleneck in the further decomposition of the amine framework. This bottleneck, in turn, is what evidently makes it possible for a major ultimate product of the nitro–nitrite rearrangement to be the nitrosamine.

In this and the following paragraphs, we consider some of the other reactions that have been previously suggested for nitrosamine formation. Beginning with the results of Fluornoy[1] some years ago, a number of suggestions have been made for the formation of dimethylnitrosamine as the main product from the thermal decomposition of dimethylnitramine. Two of these, namely unimolecular oxygen atom loss (15) and NO addition to the imine followed by scavenging of the resulting carbon-centered radical (16), can be ruled out on thermochemical grounds. Reaction

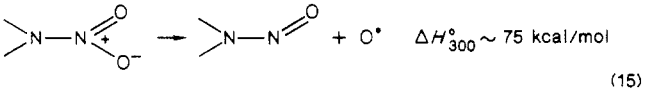

(15)

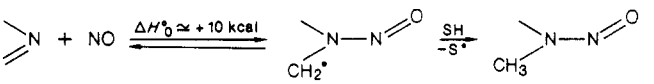

(16)

15 is not a possible explanation because it has an endothermicity[12] substantially exceeding the observed activation energy for nitrosamine production. Reaction 16 is unfavorable because the exothermic decomposition of the intermediate (reaction −16) is much faster than it stabilization by any conceivable[13] scavenger.

The remaining candidates that need to be considered include recombination of NO with the dimethylamino radical (9) as invoked by Lin,[2] radical addition to one of the nitro group oxygens as discussed by Melius[12] (12, 13) (i.e., direct biomolecular reduction of the intact nitramine), and bimolecular or unimolecular formation of the unstable *O*-nitroso compound (6, 3) as an effective route to high yields of NO to serve as an intermediate for reaction 9.

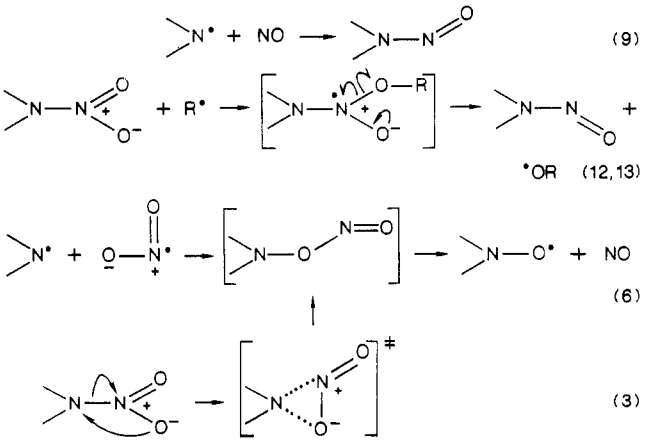

The recombination of NO with the dimethylamino radical is the logical first candidate and has been invoked by all previous workers as a major source of nitrosamine; this step can be preceded by NO production routes consisting of a sequence of "known" unimolecular and bimolecular reactions (1 and 7) and/or by the nitro–nitrite rearrangement (3) which has precedent as a unimolecular process in nitromethane[15] and nitrobenzene[16,17] de-

(15) Wodtke, A. M.; Hintsa, E. J.; Lee, Y. T. *J. Phys. Chem.* **1986**, *90*, 3549.

(16) Gonzalez, A. C.; Larson, C. W.; McMillen, D. F.; Golden, D. M. *J. Phys. Chem.* **1985**, *89*, 4809.

composition.

The four-center "recombination" leading directly to two nitrosomethane molecules suggested by Lin would appear to have steric requirements that are too stringent to be the high A factor process that is evidently required to explain his observations. On the other hand, reaction 17 is not an unreasonable suggestion on enthalpic grounds, given the known tendency[18] of C-nitroso compounds to dimerize.

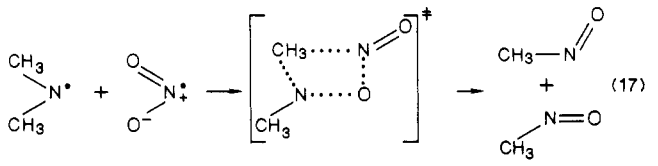

(17)

The model used by Lin successfully reproduced his observed DMNA decomposition and DMNO formation rates through a route involving almost complete oxidative fragmentation of the amino structure and formation of NO as an intermediate in rather large yields in the process. However, there are several key steps whose parameters need to be carefully assessed in order to judge the adequacy of the reaction scheme as assembled by Lin. These are the four-center recombination (17) considered above, the oxidation of the dimethylamino radical by NO_2 (7), and the thermolysis of nitrosomethane.

Reaction 17 can be viewed as a disproportionation with rather severe steric requirements. While the impact of these requirements on the rate may be tempered by the fact that the nitrosomethane dimer is bound[18] by about 17 kcal/mol, an A factor of 3×10^9 L/(m s) is still surprisingly high. Furthermore, for this reaction to take place to the exclusion of the recombination at an oxygen atom site (i.e., reaction 7), a known reaction that has no unusual steric requirements and leads to oxidation of the radical, is even more surprising. In principle, this "known" route can lead to the same products as the four-center recombination (17), since oxidation of the dimethylamino radical gives a nitroxyl radical (7), which upon β-scission, gives the methyl radical and a molecule of nitrosomethane.

$$(CH_3)_2N\text{-}O^{\bullet} \rightarrow CH_3NO + CH_3^{\bullet} \qquad (18)$$

Thermolysis of nitrosomethane then gives NO and another methyl radical, which can go on to reduce more NO_2 to NO.

$$CH_3\text{-}NO \rightarrow CH_3^{\bullet} + NO \qquad (19)$$

Whether the sequence of reactions 7, 18, and 19 will in practice give the same results as reactions 17 and 19 is another question, since nitroxyl radicals are quite stable in general, and this particular one is estimated[12] to have a methyl–N bond strength of 44 kcal/mol.

Finally, the unimolecular dissocation (19) of the nitrosomethane itself is another step at which a bottleneck must be avoided, if recombination as the sole route to nitrosomethane is to satisfactorily explain the various experimental results. The parameters that Lin[2] has evidently found necessary for this step to be fast enough include an A factor of 5×10^{16} L/(m s). Values in the literature[14] for loss of diatomic fragments, as well as consideration of the overall entropy change in this particular reaction, indicate that 5×10^{16} is about an order of magnitude too large for nitrosomethane thermolysis, without consideration of the effects of falloff. In fact, use of all the other parameters chosen by Lin, but with the A factor for this reaction lowered to 5×10^{15}, lowered the computed dimethylnitrosamine yield at 500 K from the observed 60% to 40%. These difficulties do not absolutely rule out NO recombination as the sole route to the nitrosamine but serve at least to (a) quantify the intuition that a delicate balance among secondary reactions is required in order to produce enough NO for nitrosamine production through recombination, while still leaving enough intact dimethylamino radicals to recombine with the NO, and (b) amplify Lin's original finding that a fully satisfactory explanation does not easily follow from previously documented reactions.

A nitrosamine formation route that would not require a critical balance between amino radical survival and oxidative fragmentation is the one first made by Schroeder[19] and recently subjected by Melius[12] to calculation by the BAC-MP4 method. If reaction 12 is facile enough, it will result in rapid formation of the nitrosamine from virtually any radical produced in the system.

Reactions 12 and 13 are quite reasonable: they are molecular analogues to the oxidation of radicals by NO_2. Since they are not radical–radical reactions, but radical additions to a double bond, one might expect them to exhibit activation energies types of those classes of reactions (1–2 kcal/mol for H atoms and 5–7 kcal/mol for carbon-centered radicals). However, the calculation of Melius[12] evidently suggest little or no activation energy for methyl radicals as well as for hydrogen atoms. Thus, in order to derive an upper limit to the possible importance of these reactions, we have incorporated them (for R = H$^{\bullet}$ and $CH_3^{\bullet}$) into the numerical model described above using appropriate A factors and zero activation energies for methyl radicals as well as hydrogen atoms. Under these conditions, the computation showed that reaction under the modeled temperature–time history illustrated in Figure 5 and in the presence of a 50-fold excess of toluene as radical scavenger resulted in a contribution to dimethylnitrosamine production from reactions 12 and 13 that was no more than 20% of the total yield of that product. Furthermore, the inclusion of these reactions did not lead to a tendency toward lower Arrhenius parameters. Thus, while they may be important during actual nitramine combustion, the nitrosamine formation reactions considered by Melius[12] would seem not to be responsible for the low A factors and low activation energies observed under our scavenged laser pyrolysis conditions. In other words, we cannot, by inclusion of these reactions in the model, duplicate the observed temperature dependence for DNMA loss, namely, an A factor and activation energy 2 powers of 10 and 10 kcal/mol, respectively, below those indicative of simple N–NO_2 bond scission.

Summary

The decomposition temperature dependence and the product yields in the laser pyrolysis of dimethylnitramine can be accounted for (1) by a combination of competing unimolecular bond scission and nitro–nitrite rearrangement as the initial loss reactions and (2) by a low-temperature pathway to nitrosamine that involves reversals of the nitro–nitrite rearrangement and nitrite homolysis steps, coupled with a direct route from the unstable nitrite (or its oxidation-state equivalent, the nitroxyl radical) to dimethylnitrosamine. Among these, the latter is the only reaction strictly without precedent; even it, as a displacement of NO_2 from the nitrite by NO, is somewhat analogous to radical addition to a double bond. Parameters assigned to it on this basis allow the experimental observations to be reproduced without abandoning plausibility.

These results reveal competing initial reactions and facile secondary reactions in the decomposition of a simple nitramine. Understanding the range of possible reactions is clearly a necessary part of understanding the conditions required for the decomposition of this and more complex nitramines to become thermally self-sustaining. It is entirely fitting that our attempt to further this understanding is presented as part of a tribute to Fred Kaufman, who so aptly described endeavors such as this in his seminal plenary lecture[20] to the 19th Symposium (International) on Combustion. Experiments now under way with a different LPHP apparatus, in which the initial products of laser decomposition are detected directly via molecular beam mass spectrometry, will provide ad-

(17) Tsang, W.; Robaugh, D.; Mallard, W. G. *J. Phys. Chem.* **1986**, *90*, 5968.

(18) Batt, L.; Robinson, G. N. In *Chemistry of Functional Groups: Supplement F*; Patai, S., Ed.; Wiley: Chichester, 1981; p 1035.

(19) Schroeder, M. A. In *Proceedings of the 16th JANNAF Combustion Meeting*; CPIa: 1978; Vol. *82*, p 644. 1979; Vol. 2, p 17.

(20) Kaufman, F. In *Proceedings of the 19th Symposium (International) on Combustion 1981*; The Combustion Institute: Pittsburgh, PA, 1982; p 1.

ditional information about this competition.

Acknowledgment. We acknowledge the support of the U.S. Army Research Office under Contract DAAC03-86-K-0030 and the Air Force Office of Scientific Research under Contract F49620-85-K-00006. We also thank Alicia C. Gonzalez for experimental efforts in the early part of this work. D.M.G. acknowledges the joy of having worked with and been a friend of Fred Kaufman. His enthusiasm, humor, and essential humanity are sorely missed.

Registry No. DMNA, 4164-28-7; DMNO, 62-75-9; toluene, 108-88-3; methylmethylenimine, 1761-67-7; dimethylamine, 124-40-3; *N,N*-dimethylbenzylamine, 103-83-3.

Gas-Phase Isotope-Exchange Reactions with Chloride Ion

Jane M. Van Doren, Charles H. DePuy,* and Veronica M. Bierbaum*

Department of Chemistry and Biochemistry, University of Colorado, Boulder, Colorado 80309-0215
(Received: December 7, 1987)

Gas-phase isotope-exchange reactions of $^{37}Cl^-$ have been studied in a selected ion flow tube at thermal energy. The S_N2 reaction of $^{37}Cl^-$ with methyl chloride is immeasurably slow at room temperature, indicating that the transition state is close to or projects above the energy of the reactants. In contrast, the corresponding displacement reactions with chlorotrimethylsilane and chlorodimethylphosphine are facile, indicating that reaction barriers are low and suggesting the possible formation of low-energy intermediates. Exchange with acetyl chloride occurs at a moderate rate while exchange with thionyl chloride occurs at the statistical limit; for sulfuryl chloride only chlorine atom abstraction is observed. Reaction of $^{37}Cl^-$ with molecular chlorine proceeds in half of the collisions, suggesting formation of Cl_3^- from end-on attack; the unique central atom is not exchangeable. Isotope exchange with hydrogen chloride and deuterium chloride occurs with ~50% efficiency, implicating reaction through a long-lived complex rather than by a direct mechanism.

Symmetrical exchange reactions, in which an atom or group within a molecule is replaced by an identical atom or group, have always played key roles in the elucidation of reaction mechanisms and in correlations of the effect of structure on reaction rates. Such exchange reactions also hold great potential for exploring the detailed dynamics of gas-phase ion–molecule processes. Due largely to the work of Brauman and co-workers,[1] most thermal energy gas-phase ion–molecule reactions are described by double-well potential energy surfaces, as shown in Figure 1. The ion and neutral molecule are attracted to one another to form an electrostatically bound complex [*X⁻·RX]. Reaction then proceeds through a transition state [*X···R···X]⁻ in which the rate-determining chemical transformations occur. In the final step, a complex of the ion and neutral products is formed which then separates. In the symmetrical exchange process shown in Figure 1, the reaction is thermoneutral so that the reactants and products are at the same energy as are the reactant and product complexes. Such reactions are particularly important because they allow one to make inferences about intrinsic barriers to reactions, i.e., activation energies in the absence of an energetic driving force. The height of the intrinsic barrier is expected to be very sensitive to the structure of the transition state and thus to the detailed mechanism of the reaction. As shown in Figure 1, we can envision barriers that are sufficiently low so as to have no effect on the reaction rate, barriers so high that the reaction cannot proceed at thermal energy, and, most usefully for the study of reaction dynamics, barriers of intermediate height which retard but do not prevent the reaction. Thus, a study of the rates of these symmetrical ion–molecule processes allows us to probe the nature of their reaction barriers. These reactions are also of great importance in the widening application[2] of Marcus theory[3] to the prediction of reaction rates. In this theory the rate of an unsymmetrical reaction is estimated from the intrinsic barriers of the two symmetrical processes and the overall reaction thermochemistry. By combining intrinsic barriers, reaction enthalpies, and experimental ion–neutral complexation energies, one can define many of the features of the double-minimum potential energy surfaces that describe ion–molecule reactions.

In view of the importance of symmetrical reactions, there are surprisingly few such rate coefficients available in the field of gas-phase ion chemistry, especially at thermal energies. In this paper we report the rate coefficients, measured in a selected ion flow tube, of the gas-phase exchange reactions of $^{37}Cl^-$ with methyl and acetyl chloride, chlorotrimethylsilane, chlorodimethylphosphine, thionyl and sulfuryl chloride, chlorine, and hydrogen and deuterium chloride.

Experimental Section

The rate coefficients were measured at room temperature in a selected ion flow tube (SIFT) which has been previously described.[4] The $^{37}Cl^-$ ions were formed in a low-pressure electron impact source from carbon tetrachloride, separated from the neutral precursor and other ions in a quadrupole mass filter, and injected into a flowing afterglow in which helium at 0.4 Torr was used as the buffer gas. Methyl chloride (Matheson, 99.5%), chlorine (Matheson High Purity grade, 99.5%), hydrogen chloride (Matheson Technical grade, 99.0% minimum), and deuterium chloride (MSD Isotopes, 99% minimum D) were used without further purification. Chlorotrimethylsilane (Aldrich, 98%) was distilled before use. Chlorodimethylphosphine (Strem Chemical) was distilled onto pure 1,10-phenanthroline to absorb any HCl and then distilled directly into the flow tube. Reaction with H_3O^+ showed 97% $[M + 1]^+$ of the chlorodimethylphosphine and 3% $[M + 1]^+$ of dichloromethylphosphine. Thionyl chloride (Aldrich

(1) (a) Olmstead, W. N.; Brauman, J. I. *J. Am. Chem. Soc.* **1977**, *99*, 4219. (b) Farneth, W. E.; Brauman, J. I. *J. Am. Chem. Soc.* **1976**, *98*, 7891. (c) Asubiojo, O. I.; Brauman, J. I. *J. Am. Chem. Soc.* **1979**, *101*, 3715. (d) Jasinski, J. M.; Brauman, J. I. *J. Am. Chem. Soc.* **1980**, *102*, 2906.

(2) (a) Pellerite, M. J.; Brauman, J. I. *J. Am. Chem. Soc.* **1980**, *102*, 5993. (b) Barfknecht, A. T.; Dodd, J. A.; Salomon, K. E.; Tumas, W.; Brauman, J. I. *Pure Appl. Chem.* **1984**, *56*, 1809. (c) Han, C.-C.; Dodd, J. A.; Brauman, J. I. *J. Phys. Chem.* **1986**, *90*, 471. (d) Dodd, J. A.; Brauman, J. I. *J. Phys. Chem.* **1986**, *90*, 3559.

(3) (a) Marcus, R. A. *Annu. Rev. Phys. Chem.* **1964**, *15*, 155. (b) Marcus, R. A. *J. Phys. Chem.* **1968**, *72*, 891. (c) Cohen, A. O.; Marcus, R. A. *J. Phys. Chem.* **1968**, *72*, 4249.

(4) (a) Grabowski, J. J.; DePuy, C. H.; Bierbaum, V. M. *J. Am. Chem. Soc.* **1983**, *105*, 2565. (b) Grabowski, J. J. Ph.D. Dissertation, University of Colorado, 1983.

0022-3654/89/2093-1130$01.50/0 © 1989 American Chemical Society